Constructing the Universe with Clusters of Galaxies, IAP 2000 meeting, Paris (France) July 2000
Florence Durret & Daniel Gerbal eds.

COMBINING SZ, X-RAYS AND LENSING DATA ON THE CLUSTER OF GALAXIES CL0016

F.J. CASTANDER[1], G.P. HOLDER[2], D. CLOWE[3], J.E. CARLSTROM[2], M. SCHIRMER[3], E.D. REESE[2], J.-P. KNEIB[1]
[1] *Observatoire Midi-Pyrénées, 14 Av Edouard Belin, 31400 Toulouse, France*
[2] *Department of Astronomy & Astrophysics, University of Chicago, 5640 S Ellis Ave, Chicago IL 60637, USA*
[3] *Max-Planck Institut-für-Astrophysik, 85740 Garching, Germany*

We combine observations in the optical, radio and X-rays of the cluster of galaxies CL0016 to constrain its gravitational potential. These observations include deep Keck imaging in the optical; BIMA and OVRO interferometric observations at cm wavelengths and ROSAT PSPC and HRI X-ray imaging. Each observation provides different information about the cluster: the distortions of background galaxies depend on the cluster projected potential; the Sunyaev-Zeldovich decrement, on the integrated pressure and the X-ray emission, on the square of the projected gas density (if isothermal).
We use a maximum likelihood analysis to combine these data to derive the cluster potential. We discuss different approaches to construct the likelihood functions, the different assumptions required and the current status of the project.

1 Introduction

Clusters of galaxies are a mixture of dark matter, hot gas and galaxies whose detailed structure and composition are still not fully understood. Such an understanding of the physical processes taking place in clusters and how they affect their evolution is necessary to use them as cosmological probes.

Observationally clusters can be studied from different points of view and wavelengths. For instance, optical imaging can be used to count galaxies and select clusters. One can also assign richnesses and study the cluster members' colour properties. Spectroscopic observations provide redshit determinations with which one can compute velocity dispersions. The spectra also reveal the properties of the galaxy members. In X-rays one can measure the surface brightness and temperature of the hot gas emission. Deep imaging can allow us to measure the distortions of background galaxies induced by the cluster gravitational potential. Radio observations can detect the decrement at long wavelengths in the temperature of the cosmic microwave background (CMB).

Given the different physical processes probed by those measurements, a combination of them can help us understand the physical processes taking place in them. Here, we present a method

to combine several observation at different wavelengths which we apply to the cluster of galaxies CL0016.

2 The cluster of galaxies: CL0016+16

CL0016+16 was originally discovered by Richard Kron searching photographic plates. Koo (1981) published the first optical study measuring a richness twice as large as that of the Coma cluster. A decade later, Dressler & Gunn (1992) measured a cluster redshift of $z = 0.5455$ and a velocity dispersion of $\sigma = 1324$ km/s with 30 cluster galaxy members. The CNOC group (e.g., Carlberg et al 1996) measured the redshifts of 47 extra cluster members obtaining $z = 0.5481$ and $\sigma = 1243$ km/s. They computed a mass-to-light ratio of $M/L = 260\ h^{-1}$.

In X-rays, the EMSS measured an X-ray luminosity of $L_x = 14.6 \times 10^{44} h_{50}^{-2}$ erg/s for this cluster (Gioia et al 1990). Several authors (Neumann & Böhringer 1997; Hughes & Birkinshaw 1998; Reese et al 2000) have analysed the ROSAT PSPC and HRI observations of this cluster. Fitting a standard beta model profile to the cluster emission(Eq 2), they obtain values of $\beta =$ 0.75-0.80 and $r_c =$ 40-45″. Furuzawa et al (1998) and Hughes & Birkinshaw (1998) have analysed the ASCA observations measuring a cluster temperature of $T_x \sim 8$ KeV.

Clowe et al (2000) obtained deep Keck images of this cluster which they use to reconstruct its projected mass distribution. In particular, they fit the cluster mass profile to an isothermal sphere and to a NFW profile. Both fits are statistically acceptable, the NFW being slightly better. The isothermal fit gives a velocity dispersion of ~ 800 km/s, lower than that found by the CNOC group.

Carlstrom et al (2000) observed CL0016 at the OVRO and BIMA observatories using radio interferometric techniques at cm wavelengths. Reese et al (2000) used these data in conjuction with the ROSAT X-ray data to measure the Hubble constant.

3 Methodology

We have chosen to combine the lensing, X-ray and SZ data mentioned above using a maximum likelihood method. The main idea is to constrain the cluster potential constructing a likelihood function which is the product of the likelihoods of the different observations, that is,

$$\mathcal{L}(\phi) = \mathcal{L}_{lensing}(\phi) * \mathcal{L}_{x-rays}(\phi) * \mathcal{L}_{SZ}(\phi) \tag{1}$$

and maximize that function. This formulation allows us to attack the problem for each observation separately.

Deep optical images measure the ellipticities, magnitudes and sizes of background galaxies. The reduced shear, g, can be computed from the background galaxies ellipticities. In fact, it is the expected value of the ellipticities in the weak lensing regime. The reduced shear can also be directly obtained from the second derivatives of the projected potential. Several authors have developed methods to formulate likelihood functions (or similar) for weak lensing observations. Bartelmann et al (1996) evaluate a χ^2 function comparing the reduce shear coming from observations and from the cluster potential in a grid. Seitz et al (1998) developed an entropy regularized likelihood similar to the previous method but using the ellipticities of all the background galaxies without a grid and including a regularization term. Briddle et al (1998) developed a maximum entropy method, similar to the previous one, but using a Bayesian formulation.

X-rays observations measure the surface brightness (and the temperature of the intracluster gas if enough spectral resolution is available) of the X-ray emission. The gas density can be inferred from the surface brightness and the temperature. If hydrostatic equilibrium is assumed

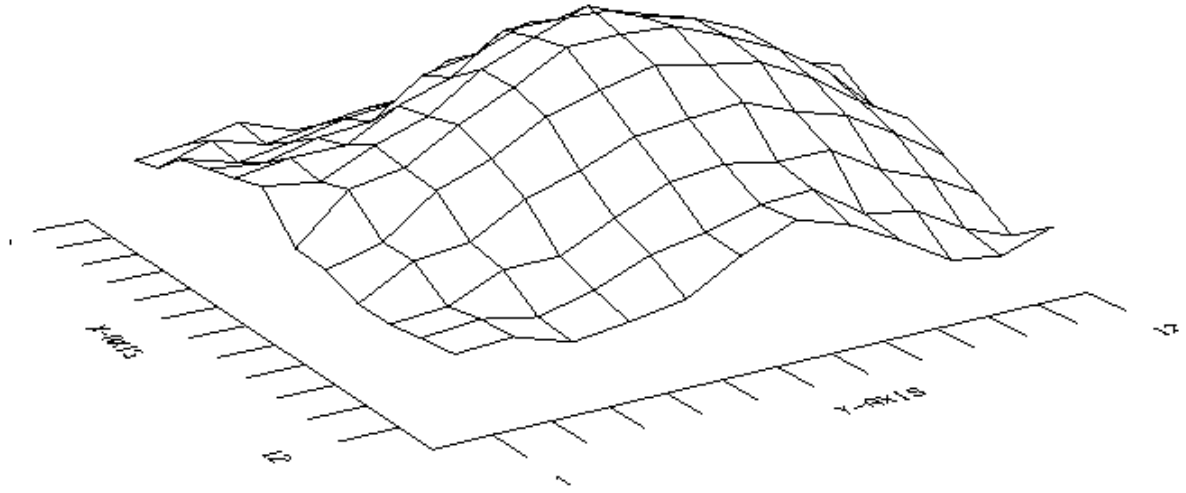

Figure 1: Non-parametric reconstruction of the CL0016 cluster projected potential using weak lensing data.

then one can obtain the cluster potential. Hughes & Birkinshaw (1998) computed a likelihood function for X-ray observations taking into account the Poissonian nature of the X-ray data.

Radio observations of the SZ effect measure the temperature decrement (at long wavelengths) of the CMB due to the hot intracluster medium. This decrement is proportional to the integrated pressure along the line of sight. Knowing the temperature, one can obtain the gas density, and assuming hydrostatic equilibrium one can get the cluster potential. The radio data available were obtained using interferometric techniques, in which one measures intensities in the u-v plane. Reese et al (2000) constructed a likelihood function which is computed in the Fourier Plane where observations are obtained.

4 Current status

We have started developing the code to compute the total likelihood function and maximize it. In our prescription the likelihood function is naturally separated into individual likelihoods coming from the different observations. Each of these is implemented as a different module.

For the weak lensing module we have implemented parametric and non-parametric methods. We have carried out simulations to check the accuracy of the cluster potential reconstruction and the biases introduced in the reconstruction.

Figure 1 shows the non-parametric reconstruction of the projected potential of cluster CL0016. The reconstructed potential is remarkably smooth. This is expected as no obvious strong lensing features are observed in this cluster in HST images.

We have also implemented the X-ray and SZ modules. The code is very similar to that of Reese et al (2000) and our results are almost indistinguishable from theirs, when fitting isothermal beta models.

We have started combining the different likelihoods. As a starting point we have chosen to use the parametric spherically symmetric beta model, where the gas density profile is given by

$$n(r) = n_0 \left(1 + \left(\frac{r}{r_c}\right)^2\right)^{-\frac{3}{2}\beta} . \qquad (2)$$

The X-ray data and SZ data are fitted to the X-ray surface brightness and temperature decrement (for their expressions see for example Reese et al 2000). Assuming isothermal hydrostatic equilibrium one can then differentiate the logarithm of the gas density and integrate to get the potential. One can then integrate along the line of sight to obtain the projected potential

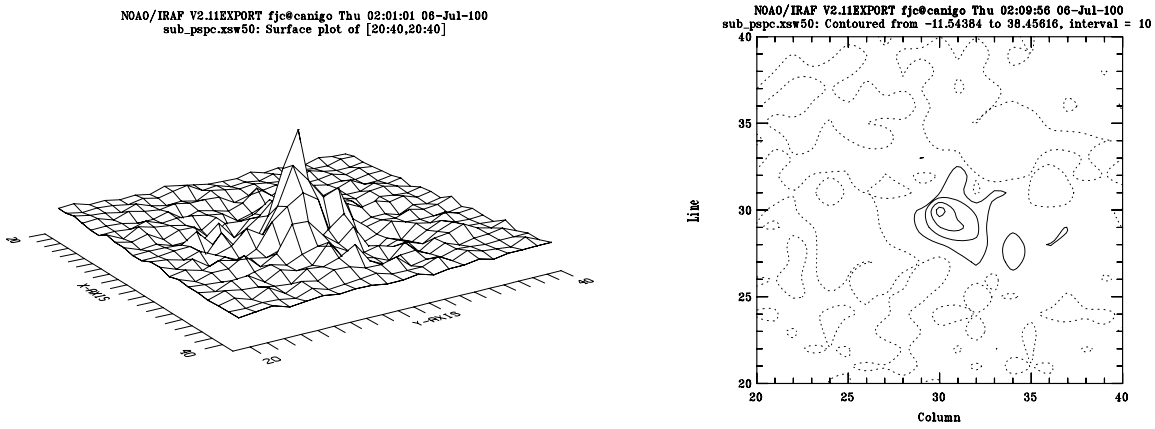

Figure 2: Difference between the cluster reconstructed potential using the PSPC X-ray data and the weak lensing data. A 3-dimensional projection (left) and the contour levels (right) are shown. Note that the X-ray reconstructed potential is more centrally concentrated.

to use for the lensing module. Preliminary results indicate that the SZ data is the least constraining data set given that the $u-v$ plane is not completely sampled by the observations. The X-ray and SZ data are consistent in describing the same gas distribution. However, the shallow potential inferred from the lensing data (under the assumptions made) requires a shallower gas distribution than that observed in X-rays and SZ. Figure 2 illustrates this point showing the difference between the cluster reconstructed potential from the X-ray PSPC data and the weak lensing data.

This project has now studied the reconstruction using the beta model parameterization. We plan to extend the comparison to other models (parametric, non-parametric, triaxial,...) and a larger cluster sample that will help us understand better the physical processes in clusters.

Acknowledgments

FJC acknowledges financial support from the TMR network of the European Commission under contract No: ERBFMRX-CT98-0172.

References

1. Bartelmann, M. et al, ApJ **464**, L115 (1996).
2. Briddle, S.L. et al, MNRAS **299**, 895 (1998).
3. Carlberg, R. G. et al, ApJ **462**, 32 (1996).
4. Carlstrom, J. et al, PhST **85**, 148 (2000).
5. Clowe, D., Luppino, G., Kaiser, N. & Gioia, I., ApJ **539**, 540 (2000).
6. Dressler, A. & Gunn, J.E., ApJS **78**, 1 (1992).
7. Furuzawa, A. et al, ApJ **504**, 35 (1998).
8. Gioia, I. et al, ApJS **72**, 567 (1990).
9. Hughes, J.P. & Birkinshaw, M., ApJ **501**, 1 (1998).
10. Koo, D., ApJ **251**, L75 (1981).
11. Neumann, D. & Böringher, H., A&A **289**, 123 (1997).
12. Reese, E.D. et al, ApJ **533**, 38 (2000).
13. Seitz, S. et al, A&A **337**, 325 (1998).